

# Fractal Fluctuations in Quiet Standing Predict the Use of Mechanical Information for Haptic Perception

ZSOLT PALATINUS,<sup>1,2</sup> JAMES A. DIXON,<sup>1,2,3</sup> and DAMIAN G. KELTY-STEPHEN<sup>4</sup>

<sup>1</sup>Department of Psychology, University of Connecticut, 406 Babbidge Road, Unit 1020, Storrs, CT 06269-1020, USA; <sup>2</sup>Center for the Ecological Study of Perception and Action, University of Connecticut, 406 Babbidge Road, Unit 1020, Storrs, CT 06269-1020, USA; <sup>3</sup>Haskins Laboratories, 300 George St., New Haven, CT 06511, USA; and <sup>4</sup>Wyss Institute for Biologically Inspired Engineering, Harvard University, 3 Blackfan Circle, 2nd Floor, Boston, MA 02115, USA

(Received 23 July 2012; accepted 15 November 2012; published online 27 November 2012)

Associate Editor Thurmon E. Lockhart oversaw the review of this article.

**Abstract**—Movement science has traditionally understood high-dimensional fluctuations as either antithetical or irrelevant to low-dimensional control. However, fluctuations incident to changeful, sometimes unpredictable stimulation must somehow reshape low-dimensional aspects of control through perception. The movement system's fluctuations may reflect cascade dynamics in which many-sized events interact nonlinearly across many scales. Cascades yield fractal fluctuations, and fractality of fluctuations may provide a window on the interactions across scale supporting perceptual processes. To test these ideas, we asked adult human participants to judge whole or partial length for unseen rods (with and without added masses). The participants' only experience with the objects came from supporting them across their shoulders during quiet standing. First, the degree of fractal temporal correlations in trial-by-trial series of planar Euclidean displacements in center of pressure (COP) significantly improved prediction of subsequent trial-by-trial judgments, above and beyond prediction by traditional predictors of haptic perception and conventional measures of COP variability. Second, comparison with linear surrogate data indicated the presence of nonlinear interactions across scale in these time series. These results demonstrate that high-dimensional fluctuations may serve a crucial role in the cascade dynamics supporting apparently low-dimensional control strategies.

**Keywords**—Movement coordination, Postural sway, Multifractality, Surrogate data, Control, Fluctuations.

## INTRODUCTION

Movement variability poses a major challenge for the movement sciences. There is at once much consistency in the patterning of coordinated movements and a great

deal of fluctuation. The number of anatomical parameters free to vary is immense, but coordinated movements appear to follow relatively few functional parameters. A prevalent notion is that low-dimensional control strategies recruit anatomical degrees of freedom as needed, to suit intentions and task constraints.<sup>3</sup> Fluctuations are reined in, recruited, and selectively unleashed for deployment of low-dimensional movement patterns.<sup>2</sup> The challenge for movement science has been weaving the consistent with the erratic into an organism that must coordinate with its environment.

This coordination requires tailoring control strategies through perception. Novel stimulation produces lower-order changes and fluctuations that percolate through the system to engender more global low-dimensional changes, such as changes in intention or in strategy.<sup>33</sup> The movement system reflects a complex interweaving of events of different scales, a veritable cascade of effects. We propose that movement variability provides a window on cascade-like dynamics governing relationships between fluctuation and control and between organism and environment. Cascades entail nonlinear dependence in which large fluctuations engender smaller fluctuations and in which smaller fluctuations support and constrain larger fluctuations over very many scales, yielding fractal patterns of fluctuation.<sup>32</sup> The fractality of fluctuations in the movement system may support the perceptual detection of information crucial for the control of biological systems.

### *Exogenous Stimulation and Endogenous Fluctuations Reflect Cascade Dynamics*

What may be counterintuitive is that the high-dimensional fluctuations in the movement system exert

Address correspondence to Damian G. Keltly-Stephen, Wyss Institute for Biologically Inspired Engineering, Harvard University, 3 Blackfan Circle, 2nd Floor, Boston, MA 02115, USA. Electronic mail: damian.stephen@wyss.harvard.edu

powerful effects on control, even when control seems so robustly low-dimensional. We may see these nonlinearities simply by applying white-noise mechanical stimulation, that is, mechanical fluctuations without any correlation over time. Such stimulation can stabilize postural sway<sup>20</sup> as well as the rhythmic oscillations underlying gait<sup>28</sup> and respiration.<sup>4</sup> In all cases, the stimulation is below conscious awareness. The nonlinearities of the movement system somehow exploit fluctuations, translating unnoticeable perturbations into more robust control. Often loosely described as “stochastic resonance,” these sometimes salutary effects of noise have proven challenging to frame within a coherent theoretical framework.<sup>15</sup> Unlike white noise, healthy fluctuations endogenous to heartbeat, interbreath, and interspike intervals are temporally correlated over long ranges of time. The variability of intervals between heartbeats, breaths, and neural spikes grows according to power-law relationships with time.<sup>18,19,31</sup> Because power-law exponents relating fluctuations to time are fractional, these fluctuations are called fractal. Fractal fluctuations in heartbeat,<sup>11</sup> interbreath,<sup>30</sup> and interspike intervals,<sup>35</sup> reflect nonlinear dependence across scales consistent with cascade dynamics.

#### *Endogenous Fluctuations in Movement: Cascade-Driven Medium for Perturbations*

Fluctuations may underwrite coordination between the movement system’s control strategies and a changeful, unpredictable environment. The fractal structure endogenous to fluctuations is flexible enough to mimic and rapidly adjust to the nonlinear, cascade-driven structure of even unpredictable perturbations.<sup>13,25,27</sup> Although white-noise stimulation supports the flow of information through the nervous system,<sup>6</sup> fractal fluctuations may support the flow of information further.<sup>16</sup> Due to the cascade-like nonlinear dependence across scales, fractal structure may vary with time, space, and fluctuation size, yielding “multifractal” fluctuations crucial to neural and cognitive dynamics coordinating movement with environment.<sup>8,10</sup> For example, strengthening and subsequent weakening of fractal fluctuations in both gaze and hand movements predicts emergence of novel control strategies in visuospatial reasoning.<sup>1,24</sup> Fractal fluctuations may be crucial for how the movement system perceives its surroundings and responds to stimulation.<sup>13</sup>

#### *Cascade Dynamics of Movement Generate Fractal Fluctuations Supporting Perceptual Use of Environmental Information*

To move smoothly through the environment, the movement system needs to match actions both to

bodily and environmental constraints. Actions such as walking and reaching require judgments on the fly as to how far and fast to extend a given limb, with or without vision. Thus, the movement system generally depends on haptic perception,<sup>33</sup> and an extensive body of research has addressed how human participants judge geometric properties (e.g., length) of objects they cannot see but can only experience haptically.<sup>34</sup> In the present section, we suggest that, similar to movement science, haptic perceptual research is caught up between complementary ways of considering perceptual exploration: low-dimensional wielding or high-dimensional fluctuations. We then discuss how fractal fluctuations endogenous to movement may moderate haptic perception.

Exploratory movements involving wielding by the hand help human participants to detect mechanical information in unseen objects. Low-dimensional rotational patterns in wielding offer up to the perceptual apparatus different elements of the mass distribution. Specifically, length judgments of unseen, wielded objects depend on moments of inertia, on-diagonal terms from the inertial tensor specifying resistance to rotation.<sup>34</sup> Judgments of partial length, that is, of segment length to either side of the grasping hand, depends on the first inertial moment  $I_{xx}$  and off-diagonal terms, e.g.,  $I_{yz}$ .<sup>5</sup> Potentially surprising is that low-dimensional wielding is not necessary. Even in static limb postures, the persisting, unintentional fluctuations support detection of mechanical information.<sup>34</sup> So, high-dimensional fluctuations embedded in exploratory movements mediate perception of mechanical distributions in a task environment.

Furthermore, the fractality of fluctuations in exploratory movement predicts how the movement system uses mechanical information for haptic perception. Research in wielding-based haptic perception has found, first, that the time series of Euclidean displacements in manual wielding trajectories exhibited long-range temporal correlations associated with fractality and, second, that trial-by-trial changes in fractality for wielding on each trial helped to predict effects of inertial properties on the trial-by-trial perceptual judgments of length.<sup>23</sup> This effect of fractal fluctuations extends to wielding by the foot instead of the hand.<sup>26</sup> Providing visual feedback on each trial following judgments leads participants to tailor their judgments over trials, and for both hand and foot wielding, the fractal fluctuations in wielding predict how well participants learn from feedback using the same limb and how well this training transfers to the untrained limb.<sup>26</sup> In both cases, fractal fluctuations in wielding promotes perceptual learning when the participant receives feedback during training blocks between pretest and posttest blocks.<sup>23,26</sup>

While previous findings suggest that greater fractality can promote perceptual learning under training by feedback, the relevance of fractality to perceptual judgments has been more generally demonstrated by testing the inclusion of full-factorial interactions with the already full-factorial interactions of task properties, inertial properties, and conventional measures (i.e., mean and standard deviation) of exploratory fluctuations. Given that perception and action may depend on interactions across many scales,<sup>33</sup> effects of fractality in this domain will not likely be limited to simple main effects and lower-order interactions. This full-factorial approach keeps the inquiry conservative, saturating the model with all likely predictors. Before parsing these immense models into significant effects, it is important first to establish that fractality is a key factor after controlling for all interactions of conventionally relevant experimental details. Because we will not provide feedback in this quiet-standing haptic task, we do not expect fractality to predict better perceptual learning and improved accuracy. Rather, because increased fractality indicates the weakening of constraints for exploring new relational structure and because feedback can diminish fractal fluctuations,<sup>1,8,14</sup> we may predict that fractality will simply increase across the span of the experiment.

We now test the perceptual relevance of fractal fluctuations under conditions in which the intended low-dimensional movement is minimal. Recent work in haptic perception has shown that wielding by the torso (i.e., intentionally swaying one's stance about the hips) yields comparable perceptual judgments as those following wielding by the hand.<sup>17</sup> We now test haptic perceptual judgments following the torso's equivalent to static holding, namely, quiet standing. Previous perceptual work has only examined fractal fluctuations in wielding by freely moving limbs. Whereas freely moving limbs can be dedicated to wielding with the intention to perceive, quiet stance may itself enlist so many attentional and physiological constraints as to dissociate incident postural fluctuations from fluctuations for perception. Hence, examining haptic perception in quiet standing allows an intriguing test of the effects of fluctuations in the movement system.

### *Hypotheses*

Given the findings of cascade dynamics through the movement system,<sup>10–12,25,30,35</sup> we expect that the movement system's fractal fluctuations will influence perceptual judgments even when they are incidental to whole-body stabilization, and we will test three hypotheses following from this expectation. The fluctuations in COP during quiet standing have been shown to be fractal.<sup>9</sup> Our first hypothesis is that the

fractal temporal correlation of Euclidean displacements in COP during quiet standing moderates the effect of mechanical information for haptic perceptual judgments of length for unseen objects. We will examine haptic perceptual judgments of whole and partial length in order to make this test more general: we expect that fractality will improve predictions of perceptual length already accounting for key inertial properties and conventional measures of postural variability above and beyond partial- or whole-length task differences in the haptic-perceptual task. Our second hypothesis is that, in the absence of feedback, fractality will increase over the course of the experiment. Our third hypothesis is that fractality of Euclidean displacements in COP reflect the nonlinear interactions across scales found in cascade dynamics. Specifically, we will compare the multifractality against linear surrogate time series, and we predict a significant difference between multifractality of original series and that of surrogate series.

## METHOD

### *Participants, Apparatus, and Procedure*

Fourteen adult participants provided informed consent according to the University of Connecticut institutional review board and the Declaration of Helsinki.

Center of pressure (COP) data were collected by using an AMTI force platform (Advanced Mechanical Technology, Inc., Watertown, MA, USA) and a 64-channel Run Technologies (Mission Viejo, CA) Datapac 2000 analog-to-digital collection system. The force fluctuations were sampled at a rate of 100 Hz.

Wooden rods (2.54-cm diameter) cut in three lengths (Table 1) were secured across the center of the participant's seventh cervical vertebra with a hollow PVC tube (12-cm diameter) attached to shoulder straps. Blinders worn around the head occluded visual information about the rods (Fig. 1).

**TABLE 1. Stimulus details regarding lengths and placement of weighting.**

Rod length (cm)	Placement of weighting
72	None
72	Left end
72	Right end
96	None
96	Left end
96	Right end
120	None
120	Left end
120	Right end

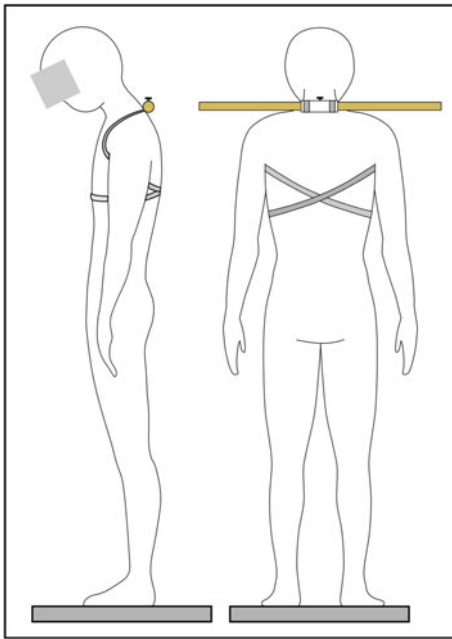


**FIGURE 1.** Schematic of experimental apparatus shown from the left side (left panel) and from behind (right panel). Rods were affixed at the participant's seventh cervical vertebra using 12-cm hollow PVC tube by straps over the shoulders, crossing the back and tied in front. Blinders blocking peripheral vision prevented participants from seeing the rods. Gray rectangles below the feet represent the force plate.

On each trial, recording started after the rod was secured in the PVC tube. Participants were instructed to stand still, judge the rod's length, and to step off the plate with their right foot when prepared to register a response (this movement marked the end of this phase and was omitted from subsequent data analysis). The response marker was positioned on a plank (2' × 4') supported 130 cm above the ground and 250 cm in front of the participant. In partial-length trials, the zero point on the plank aligned with the participant's mid-line; in whole-length trials, it was 80 cm to the participant's left. Participants directed the experimenter to adjust the response marker so that its distance from the 0-cm position matched the perceived length (whole or partial) of the attached rod until satisfied with their judgment. The same rods were used for whole and partial length judgments. Partial judgments addressed the extent of the rod from its center at the participant's spine to its extent to the participant's left-hand side. The participant could move the marker to any distance between 0 and 160 cm in partial-length trials and between 0 and 320 cm in whole-length trials. The participant used the marker to register the rod's perceived length on each trial, and the experimenter recorded the marker's distance from the zero point and reset it to the zero point at the end of each trial. Participants had no practice trials, no feedback concerning

accuracy, and only haptic information about the stimuli.

Each participant completed 27 blocked trials for both the whole-length and partial-length tasks, with order of task counterbalanced across participants. 18 trials in each task involved perception of rods weighted with a 150-g mass placed  $1/8 L$  from the rod's end, with weighted side counterbalanced and weighting randomized within block (Table 1).

### Analyses

Data analysis involved three methods, namely, detrended fluctuation analysis (DFA), growth curve modeling (GCM), and comparison of multifractal-spectrum widths for original series with multifractal-spectrum widths for iterative amplitude-adjusted Fourier transform (IAAFT) surrogates.<sup>21</sup> DFA and GCM helped to test the first and second hypotheses. DFA estimated fractal-scaling exponents  $H$  for the series of planar Euclidean displacements (PED) in COP. GCM tested whether this scaling exponent  $H$  significantly improves prediction of perceptual judgment above and beyond inertial properties, task properties, and conventional measures of postural variability. Comparison with IAAFT surrogates served to test the PED time series for cascade dynamics.

### Detrended Fluctuation Analysis

DFA assesses the strength of temporal correlations in a time series.<sup>18</sup> For time series  $x(t)$  of length  $N$ , the first step of DFA is to integrate  $x(t)$  into a random-walk trajectory  $y(t)$ :

$$y(t) = \sum_{i=1}^N x(i). \quad (1)$$

Next, linear trends  $y_n(t)$  are fitted to nonoverlapping  $n$ -length windows of  $y(t)$ . The average root mean-square (RMS) error for window sizes yields fluctuation function  $F(n)$ :

$$F(n) = \sqrt{(1/N) \sum [y(t) - y_n(t)]^2} \quad (2)$$

for  $n < N/4$ . On standard scales,  $F(n)$  is a power law

$$F(n) \sim n^H, \quad (3)$$

where  $H$  is the scaling exponent.<sup>12,18</sup> Temporally uncorrelated series yield  $H \approx .5$ , but scaling exponents in the range  $.5 < H \leq 1$  indicate long-range temporal correlations associated with fractal scaling, with stronger fractal scaling yielding exponents closer to  $H = 1$ .  $H$  can be estimated as the slope from the logarithmic scaling of Eq. (3):

$$\log F(n) \sim H \log n. \quad (4)$$

A customary test that fractal-ranged  $H$  reflects temporal correlations is to compare DFA results for the original series with results for the same numbers in shuffled order. An estimated  $H$  reflects temporal correlations when it exceeds that of the shuffled series'  $H$ .

### Growth Curve Modeling

GCM is a regression method ideal for testing the effects of time-varying predictors on longitudinal data, effective for studying trial-by-trial responses in perceptual learning.<sup>23,26</sup> Because GCM uses maximum likelihood (ML) estimation, improvement in model fit is assessed not as change in R-squared but as changes in a deviance statistic ( $-2$  times the log-likelihood [LL]) between two nested models, in which one model contains all terms in the other. When adding  $m$  predictors, the change in  $-2$  LL is tested as a chi-square ( $\chi^2$ ) with  $m$  degrees of freedom. Significantly large  $\chi^2$  indicates significantly improved prediction.<sup>22</sup>

The dependent measure of GCM was perceived length. The predictors included inertial properties (i.e.,  $I_{xx}$  and  $I_{yz}$ ), task (i.e., 1 or 0 when judgments are of partial or whole length, respectively), trial number within block (i.e., 1–27), block number, mean<sub>PED</sub>, SD<sub>PED</sub> (i.e., sample mean and sample standard deviation of PED of COP, respectively), SD<sub>AP</sub>, and SD<sub>ML</sub> (sample standard deviation of anterior–posterior [AP] and mediolateral [ML] positions, respectively), and  $H$ .

### Comparison of Multifractal Spectrum with IAAFT Surrogate Comparison

Different-sized fluctuations within the same time series may exhibit different temporal correlations. So, time-series fluctuations may be multifractal as opposed to simply fractal. Incorporating a parameter  $q$  to accentuate gradually different-sized fluctuations in the same time series generalizes DFA into a test for multifractality.

$$F(q, n) = \left[ \frac{1}{N} \sum_{v=1}^N \left\{ [y(t) - y_n(t)]^2 \right\}^{q/2} \right]^{1/q} \quad (5)$$

$$F(q, n) \sim n^{H(q)}, \quad (6)$$

$$\log F(n) \sim H(q) \log n, \quad (7)$$

where Eqs. (2), (3), and (4) equal Eqs. (5), (6), and (7) when  $q = 2$ .  $H(q)$  generalizes scaling exponent  $H$ , with  $H(q)$  for greater and lesser  $q$  reflect larger and smaller fluctuations, respectively. Because multifractal DFA can be unstable for negative values of  $q$ , we computed

multifractal DFA for  $.5 \leq q \leq 50$ , incrementing  $q$  by .5. A Legendre transformation of  $H(q)$  yields a “multifractal spectrum” of fractional values  $\alpha(q)$ , as in

$$\alpha(q) = H(q) + qH'(q). \quad (8)$$

whereas  $H(2)$  indexes fractality, the width of  $\alpha(q)$  is a crucial indicator of multifractality.<sup>10–12</sup> We included only those values of  $\alpha(q)$  for which the corresponding  $H(q)$  was estimated from a fluctuation function with correlation coefficient  $r \geq .99$ .

Multifractal analysis of original series and of the original series' IAAFT surrogate allows a test for cascade dynamics. IAAFT surrogates preserve the linear features (i.e., mean, variance, and autocorrelation) of an original series while destroying the original series's sequence. These surrogates are produced by taking the inverse Fourier transform of the original series' amplitude spectrum and a shuffled version of its phase spectrum, replacing the rank-ordered values of the resulting series with the rank-ordered values of the original series, and repeating iteratively until the rank-order replacement leaves the original amplitude spectrum intact. Testing our third hypothesis of cascade dynamics involves multifractal analysis of the original series and a sample of its IAAFT surrogates. A significant difference between an original series's multifractal spectrum from that of IAAFT is evidence of nonlinear interactions across many scales.<sup>10–12</sup>

## RESULTS

### Raw COP Data and Planar Euclidean displacement (PED) Time Series

COP series (Fig. 2, top panel) yielded PED series as the distance between consecutive pairs of COP positions (Fig. 2, bottom panel). Fourteen participants completing 27 trials in two tasks generated 756 (i.e.,  $14 \times 27 \times 2$ ) PED series. Ten trials were excluded due to unanticipated, large movements (e.g., sneezing or coughing). The remaining 746 PED series had average duration of 813.25 values (SE = 12.92), within the range of acceptable series length for DFA.<sup>7</sup>

DFA estimated trial-by-trial  $H$  for PED series ( $M = .82$ , SE = .007) in the fractal range, exceeding  $H$  for shuffled versions ( $M = .47$ , SE = .002), paired-samples  $t(745) = 43.90$ ,  $p < .001$  (e.g., Fig. 3). These results are not spuriously due to the force plate's sampling rate. Downsampling original series to produce 50- and 25-Hz series yielded  $H$  also in the fractal range ( $M = .76$  and  $.70$ , SE = .008 and .008). Effects in models reported below replicated for both downsamplings'  $H$  estimates, with final model predictions (Step 5) agreeing with original- $H$  model,  $r = .997$  and  $.992$ .

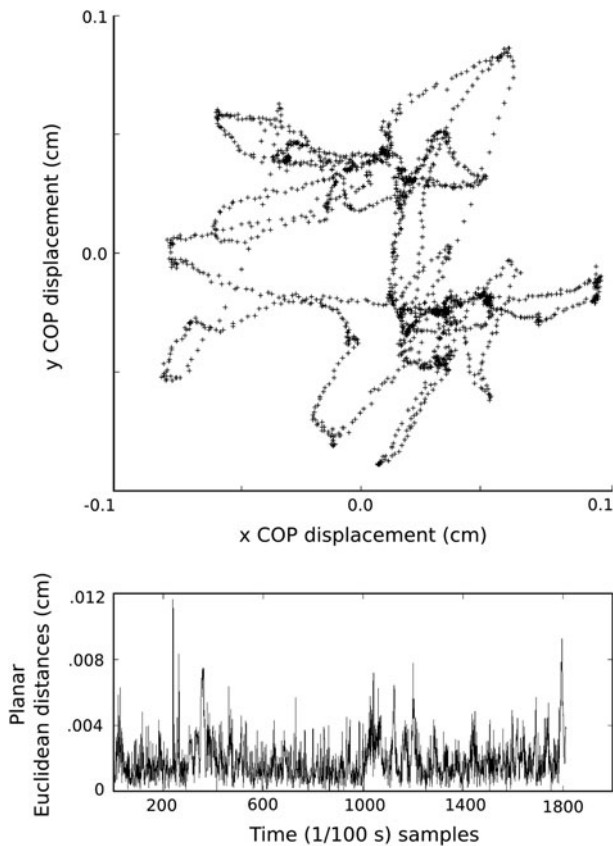


**FIGURE 2.** Example data from a single trial from a single participant leading up to a length judgment. The top panel shows the planar trajectory of the center of pressure (COP) during quiet standing sampled at 100 Hz. The bottom panel shows the corresponding time series of planar Euclidean distances (PED) separating each consecutive point in the top panel.

### Hypothesis 1 Effect of trial-by-trial fractality on haptic judgments during quiet standing

Figure 4 shows average length judgment by to-be-perceived length.

There were four main steps in building a GCM of trial-by-trial judgments. Table 2 summarizes these steps in terms of the highest-order interactions (Note: each step included all component lower-order interactions and main effects). Step 1 is the base model using the inertial properties of the rods and the interaction  $I_{yz} * \text{task}$ .<sup>5</sup> Step 2 includes block number, trial number within block, and their interactions with predictors from Step 1. Step 3 incorporated conventional measures of COP fluctuation ( $SD_{AP}$  and  $SD_{ML}$ ; and  $\text{mean}_{PED}$  and  $SD_{PED}$ ). This ensures that effects of trial-by-trial fractality (in Step 4) are not reducible to effects of simply “moving more” or “moving more variably.”

Table 2 shows  $\chi^2$  test statistics for model improvement at all steps beyond the base model. The crucial  $\chi^2$  test statistics were those for Steps 4a,  $\chi^2(80) = 141.83$ ,  $p < .0001$ , and 4b,  $\chi^2(80) = 122.61$ ,  $p < .01$ , incorporating  $H$  and its interactions with predictors from Steps

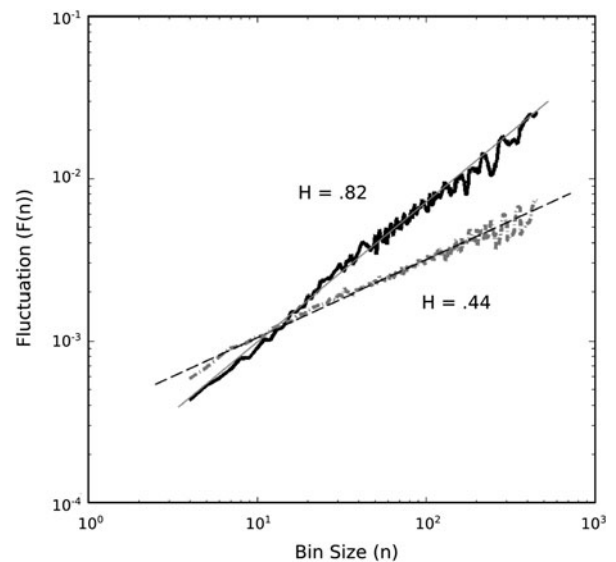


**FIGURE 3.** Fluctuation functions for a single planar Euclidean distance (PED) time series (black) and for a series of the same numbers in shuffled order (grey, dashed). The linear fit for the original series's fluctuation function has a slope of  $H = .82$ . The linear fit for the shuffled series's fluctuation function has a slope of  $H = .44$ .

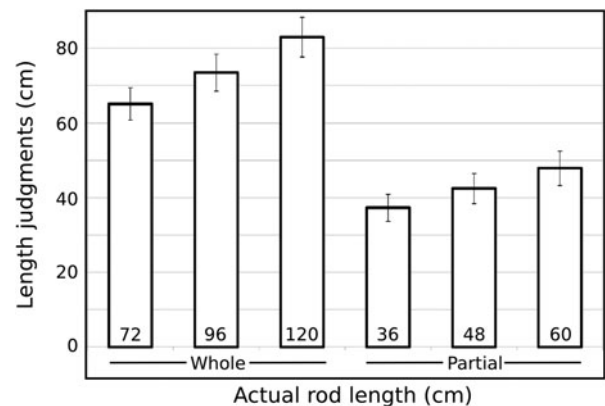


**FIGURE 4.** Length judgments depicted by average perceived length sorted by task and by length to be judged.

3a and 3b, respectively. That is, trial-by-trial  $H$  helps to predict the use of inertial properties for generating haptic perceptual judgments. Table 3 shows correlations between actual judgments and predictions from Step 4b; Fig. 5 illustrates this comparison. Table 2 also includes further modeling combining Steps 3a and 3b and confirming again that effects of  $H$  persist even after including conventional measures of postural variability. Table 4 lists significant unique effects of the last model in Step 5 (a subset of 280 effects). These effects indicate unique interactions of  $H$  with  $I_{xx}$  but not  $I_{yz}$ . However, significant interactions of  $H$  and  $I_{yz}$  may be statistically overshadowed by null higher-order interactions. Judgments showed no main effect of  $H$ .

**TABLE 2. Chi-square statistics indicating improvement in prediction with each step of growth curve modeling.**

Step	Predictors	$\chi^2$	df	$p$
1	$I_{xx} + I_{yz} * \text{Task}$			
2	$I_{xx} * \text{Block} * \text{Trial} + I_{yz} * \text{Task} * \text{Block} * \text{Trial}$	31.84	15	<.01
3a	$I_{xx} * \text{Block} * \text{Trial} * \text{SD}_{AP} * \text{SD}_{ML} + I_{yz} * \text{Task} * \text{Block} * \text{Trial} * \text{SD}_{AP} * \text{SD}_{ML}$	106.55	60	<.001
3b	$I_{xx} * \text{Block} * \text{Trial} * \text{Mean}_{PED} * \text{SD}_{PED} + I_{yz} * \text{Task} * \text{Block} * \text{Trial} * \text{Mean}_{PED} * \text{SD}_{PED}$	167.59	60	<.0001
4a	$I_{xx} * \text{Block} * \text{Trial} * \text{SD}_{AP} * \text{SD}_{ML} * H + I_{yz} * \text{Task} * \text{Block} * \text{Trial} * \text{SD}_{AP} * \text{SD}_{ML} * H$	141.83	80	<.0001
4b	$I_{xx} * \text{Block} * \text{Trial} * \text{Mean}_{PED} * \text{SD}_{PED} * H + I_{yz} * \text{Task} * \text{Block} * \text{Trial} * \text{Mean}_{PED} * \text{SD}_{PED} * H$	122.61	80	<.01
3c	$I_{xx} * \text{Block} * \text{Trial} * \text{SD}_{AP} * \text{SD}_{ML} + I_{yz} * \text{Task} * \text{Block} * \text{Trial} * \text{SD}_{AP} * \text{SD}_{ML}$ + $I_{xx} * \text{Block} * \text{Trial} * \text{Mean}_{PED} * \text{SD}_{PED} + I_{yz} * \text{Task} * \text{Block} * \text{Trial} * \text{Mean}_{PED} * \text{SD}_{PED}$	180.86 <i>Compared with 3a</i> 119.82 <i>Compared with 3b</i>	80	<.0001
4c	$I_{xx} * \text{Block} * \text{Trial} * \text{SD}_{AP} * \text{SD}_{ML} * H + I_{yz} * \text{Task} * \text{Block} * \text{Trial} * \text{SD}_{AP} * \text{SD}_{ML} * H$ $I_{xx} * \text{Block} * \text{Trial} * \text{Mean}_{PED} * \text{SD}_{PED} + I_{yz} * \text{Task} * \text{Block} * \text{Trial} * \text{Mean}_{PED} * \text{SD}_{PED}$	126.24 <i>Compared with 3c</i>	80	<.001
5	$I_{xx} * \text{Block} * \text{Trial} * \text{SD}_{AP} * \text{SD}_{ML} * H + I_{yz} * \text{Task} * \text{Block} * \text{Trial} * \text{SD}_{AP} * \text{SD}_{ML} * H$ $I_{xx} * \text{Block} * \text{Trial} * \text{Mean}_{PED} * \text{SD}_{PED} * H + I_{yz} * \text{Task} * \text{Block} * \text{Trial} * \text{Mean}_{PED} * \text{SD}_{PED} * H$	111.87 <i>Compared with 4c</i>	60	<.0001

**TABLE 3. Correlation coefficients for relationship between actual judgments and Step 4b predictions.**

Participant	$r$
1	.88
2	.74
3	.94
4	.87
5	.94
6	.94
7	.97
8	.83
9	.83
10	.90
11	.90
12	.75
13	.90
14	.92

**Hypothesis 2** Increase in fractality across trials in the absence of feedback

In the absence of feedback, fractality increased over all 54 trials. Table 5 lists coefficients for a GCM of  $H$  as a function of “trial54” (defined as trial number from 1 to 54) and Task. Trial54 led to greater  $H$  ( $B = .0032$ ,  $SE = .0009$ ,  $p < .01$ ).

**Hypothesis 3** Comparing original multifractal spectra those for IAAFT surrogates

We tested whether fractality resulted from nonlinear interactions across scales as in cascade dynamics. 628 of 746 (i.e., 84.18%) PED series exhibited multifractal spectra with ranges of  $\alpha(q)$  significantly different from those for samples of 50 corresponding IAAFT surrogates, more often than chance (i.e., 50%),  $\chi^2(1) = 348.66$ ,  $p < .0001$ .

## DISCUSSION

We predicted that fractality of fluctuations in quiet stance would (1) contribute to haptic perception,

(2) increase across trials without feedback, and (3) indicate cascade-like nonlinear interactions across scales. Results were consistent with all hypotheses.

High-dimensional fluctuations are key evidence of the cascade structure of the movement system. Fluctuations serve to support the relationship between control and changing environmental structure. The fractality of fluctuations moderates the movement system’s detection of mechanical information (e.g., inertial properties) for haptic perception. This moderating effect is not simply incidental to low-dimensional wielding movements<sup>23,26</sup> but extends to static postures. That postural fluctuations poise the movement system to detect perceptual information even as it stands in place is not a new point.<sup>29</sup> The new point is that fractality is a key property of these fluctuations.

The relevance of fractality to perception and control may point to the deeper cascade dynamics at play in the movement system. The cascade structure of temporal variation in COP fluctuations may thus entail that large postural excursions engender smaller postural excursions and in which smaller postural excursions in turn support and constrain larger fluctuations over very many scales. When we consider the dynamics of coordinated movement and try to find a place for movement variability, it is not enough to respect the traditional divide between low-dimensional control strategies and high-dimensional fluctuations. The causal contingencies likely spread more messily across the scales of analysis. Small events such as tremor and twitch may not be so negligible when considering the smooth and seemingly well-behaved, low-dimensional stuff of control. The fractal patterning of fluctuations in the movement system does not reflect the sum of independent factors following a similar, scale-invariant pattern but rather a cascading network of nonlinearly interwoven events. Fractality thus emerges from the interplay of events spreading across multiple scales of the movement system at once. It suggests that these

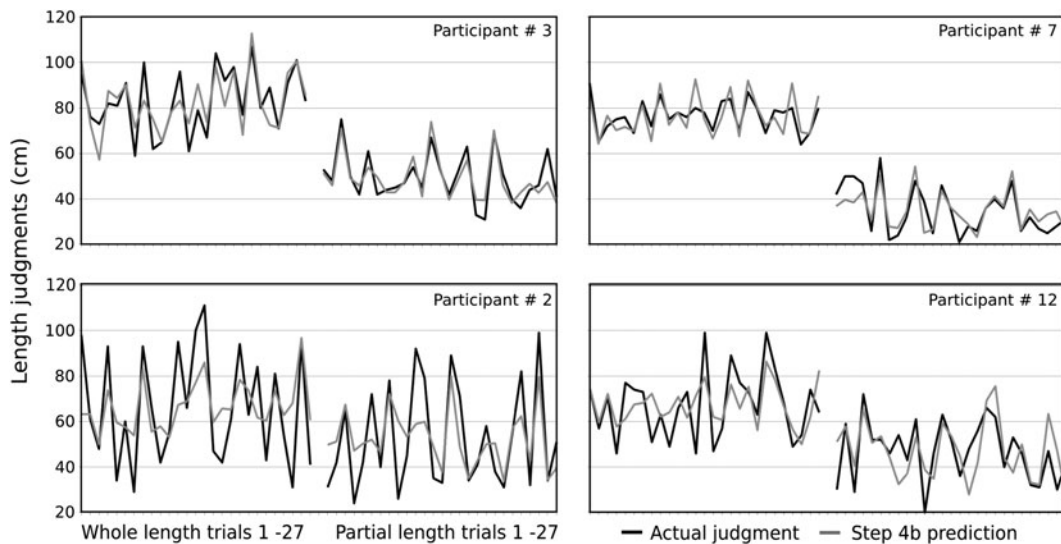


**FIGURE 5.** Comparison of actual length judgments for four example participants with model predictions from Step 4b, showing the participants for whom model predictions correlated with the two highest and the two lowest correlation coefficients  $r$ . Panels include the partial- and whole-length judgments in the order that each participant completed the task. Note that partial-length judgments are systematically lower than whole-length judgments. Model predictions from Step 4b (grey lines) shown in the figure correlated with actual judgments (black lines) as follows,  $r = .94$  (top-left panel),  $r = .97$  (top-right panel),  $r = .74$  (bottom-left panel), and  $r = .75$  (bottom-right panel). These correlation coefficients indicate the strength of a linear relationship between perceptual judgments and what the model predicts following inclusion of  $H$  and its interactions with all terms in Step 3b.

**TABLE 4.** Significant unique effects from model in Step 5.

Predictors	$B$	SE	$p$
<i>Significant unique effects excluding fractality</i>			
$I_{xx} * SD_{AP}$	.0151	.0072	<.0001
$I_{xx} * SD_{ML}$	-.0140	.0068	<.05
$SD_{AP} * SD_{ML}$	-194,700.0000	87,930.0000	<.05
$I_{xx} * Block * SD_{AP}$	-.0117	.0041	<.01
$Trial * SD_{AP} * SD_{ML}$	10,740.0000	4933.0000	<.05
$I_{xx} * Trial * Mean_{PED}$	-.0512	.0200	<.05
$I_{xx} * Mean_{PED} * SD_{PED}$	-189.7000	54.3100	<.01
$I_{xx} * Block * Trial * SD_{AP}$	.0005	.0002	<.05
$Trial * SD_{AP} * SD_{ML} * Task$	-5610.0000	2385.0000	<.05
$I_{xx} * Block * Mean_{PED} * SD_{PED}$	94.9100	29.9700	<.01
$I_{xx} * Trial * Mean_{PED} * SD_{PED}$	12.8900	3.3380	<.0001
$I_{xx} * Block * Trial * Mean_{PED} * SD_{PED}$	-6.3940	1.8550	<.01
<i>Significant unique effects including fractality</i>			
$I_{xx} * SD_{AP} * H$	-.0159	.0072	<.0001
$I_{xx} * SD_{ML} * H$	.0175	.0075	<.05
$SD_{AP} * SD_{ML} * H$	206,000.0000	81,330.0000	<.05
$I_{xx} * Block * SD_{AP} * H$	.0118	.0042	<.0001
$I_{xx} * Block * SD_{ML} * H$	-.0093	.0042	<.01
$I_{xx} * Trial * SD_{ML} * H$	-.0009	.0004	<.05
$Trial * SD_{AP} * SD_{ML} * H$	-11,520.0000	4538.0000	<.05
$I_{xx} * Trial * Mean_{PED} * H$	.0552	.0231	<.05
$I_{xx} * Mean_{PED} * SD_{PED} * H$	182.3000	49.0400	<.0001
$I_{xx} * Block * Trial * SD_{AP} * H$	-.0005	.0003	<.05
$I_{xx} * Block * Trial * SD_{ML} * H$	.0005	.0002	<.05
$Task * Trial * SD_{AP} * SD_{ML} * H$	5815.0000	2289.0000	<.01
$I_{xx} * Block * Mean_{PED} * SD_{PED} * H$	-90.8300	27.1400	<.01
$I_{xx} * Trial * Mean_{PED} * SD_{PED} * H$	-12.6300	3.0220	<.0001
$I_{xx} * Block * Trial * Mean_{PED} * SD_{PED} * H$	6.2810	1.6840	<.0001



**TABLE 5. Model testing increase of fractality across all 54 trials of the experiment.**

Predictors	<i>B</i>	SE	<i>p</i>
Intercept	.7429	.0869	<.0001
Trial54	-.0140	.0008	<.01
Task	-.0075	.0544	.89

nonlinear interactions across scales are crucial for the movement system to operate smoothly within a changing context. The fractality—and more broadly, multifractality—of cascade dynamics is essentially a statistical snapshot catching the movement system in the act of coordinating low-dimensional, relatively stable patterns and plans with the high-dimensional, relatively fleeting field of perturbations and stimulations.

### ACKNOWLEDGMENTS

The authors thank M. T. Turvey for helpful discussions, J. G. Holden and two anonymous reviewers for their helpful comments, and acknowledge NSF grant BCS-0925373 and the Wyss Institute for financial support.

### CONFLICT OF INTEREST

The authors have no conflicts of interests related to and reap no financial benefits from presenting the work reported in the manuscript.

### REFERENCES

- <sup>1</sup>Anastas, J. R., D. G. Stephen, and J. A. Dixon. The scaling behavior of hand motions reveals self-organization during an executive-function task. *Phys. A* 390:1539–1545, 2011.
- <sup>2</sup>Berniker, M., A. Jarc, E. Bizzi, and M. C. Tresch. Simplified and effective motor control based on muscle synergies to exploit musculoskeletal dynamics. *Proc. Nat. Acad. Sci. USA* 106:7601–7606, 2009.
- <sup>3</sup>Bernstein, N. A. *The Coordination and Regulation of Movements*. Oxford: Pergamon Press, p. 196, 1967.
- <sup>4</sup>Bloch-Salisbury, E., P. Indic, F. Bednarek, and D. Paydarfar. Stabilizing immature breathing patterns of preterm infants using stochastic mechanosensory stimulation. *J. Appl. Physiol.* 107:1017–1027, 2009.
- <sup>5</sup>Carello, C., M.-V. Santana, and G. Burton. Selective perception by dynamic touch. *Percept. Psychophys.* 58:1177–1190, 1996.
- <sup>6</sup>Collins, J. J., T. T. Imhoff, and P. Grigg. Noise-enhanced tactile sensation. *Nature* 383:770, 1996.
- <sup>7</sup>Delignières, D., S. Ramdani, L. Lemoine, K. Torre, M. Fortes, and G. Ninot. Fractal analyses for “short” time

- series: a re-assessment of classical methods. *J. Math. Psychol.* 50:525–544, 2006.
- <sup>8</sup>Dixon, J. A., J. G. Holden, D. Mirman, and D. G. Stephen. Multifractal dynamics in the emergence of cognitive structure. *Topics Cogn. Sci.* 4:94–102, 2012.
  - <sup>9</sup>Duarte, M., and V. M. Zatsiorsky. Long-range temporal correlations in human standing. *Phys. Lett. A* 283:124–128, 2001.
  - <sup>10</sup>Ihlen, E. A. F., and B. Vereijken. Interaction-dominant dynamics in human cognition: beyond  $1/f^\alpha$  fluctuation. *J. Exp. Psychol. Gen.* 139:436–463, 2010.
  - <sup>11</sup>Ivanov, P. Ch., L. A. N. Amaral, A. L. Goldberger, S. Havlin, M. G. Rosenblum, H. E. Stanley, and Z. R. Struzik. From  $1/f$  noise to multifractal cascades in heart-beat dynamics. *J. Nonlinear Sci.* 11:641–652, 2001.
  - <sup>12</sup>Kantelhardt, J. W., S. A. Zschiegner, E. Koscielny-Bunde, S. Havlin, A. Bunde, and H. E. Stanley. Multifractal detrended fluctuation analysis of nonstationary time series. *Phys. A* 316:87–114, 2002.
  - <sup>13</sup>Kelty-Stephen, D. G., and J. A. Dixon. Temporal correlations in postural sway moderate effects of stochastic resonance on postural stability. *Hum. Mov. Sci.* (in press).
  - <sup>14</sup>Kuznetsov, N. A., and S. Wallot. Effects of accuracy feedback on fractal characteristics of time estimation. *Front. Integr. Neurosci.* 5:62, 2011.
  - <sup>15</sup>McDonnell, M. D., and D. Abbott. What is stochastic resonance? Definitions, misconceptions, debates, and its relevance to biology. *PLoS Comp. Biol.* 5:e1000348, 2009.
  - <sup>16</sup>Nozaki, D., J. J. Collins, and Y. Yamamoto. Mechanism of stochastic resonance enhancement in neuronal models driven by  $1/f$  noise. *Phys. Rev. E* 60:4637–4644, 1999.
  - <sup>17</sup>Palatinus, Zs., C. Carello, and M. T. Turvey. Principles of part-whole selective perception by dynamic touch extend to the body. *J. Mot. Behav.* 43:87–93, 2011.
  - <sup>18</sup>Peng, C.-K., S. Havlin, H. E. Stanley, and A. L. Goldberger. Quantification of scaling exponents and crossover phenomena in nonstationary heartbeat time series. *Chaos* 5:82–87, 1995.
  - <sup>19</sup>Peng, C.-K., J. E. Mietus, Y. Liu, C. Lee, J. M. Hausdorff, H. E. Stanley, A. L. Goldberger, and L. A. Lipsitz. Quantifying fractal dynamics of human respiration: age and gender effects. *Ann. Biomed. Eng.* 30:683–692, 2002.
  - <sup>20</sup>Priplata, A. A., J. B. Niemi, J. D. Harry, L. A. Lipsitz, and J. J. Collins. Vibrating insoles and balance control in elderly people. *Lancet* 362:1123–1124, 2003.
  - <sup>21</sup>Schreiber, T., and A. Schmitz. Improved surrogate data for nonlinearity tests. *Phys. Rev. Lett.* 77:635–638, 1996.
  - <sup>22</sup>Singer, J. D., and J. B. Willett. *Applied Longitudinal Data Analysis*. New York: Oxford University Press, p. 644, 2003.
  - <sup>23</sup>Stephen, D. G., R. Arzamarski, and C. F. Michaels. The role of fractality in perceptual learning: exploration in dynamic touch. *J. Exp. Psychol. Hum. Percept. Perform.* 36:1161–1173, 2010.
  - <sup>24</sup>Stephen, D. G., R. A. Boncoddo, J. S. Magnuson, and J. A. Dixon. The dynamics of insight: mathematical discovery as a phase transition. *Mem. Cogn.* 37:1132–1149, 2009.
  - <sup>25</sup>Stephen, D. G., and J. A. Dixon. Strong anticipation: multifractal cascade dynamics modulate scaling in synchronization behaviors. *Chaos Solitons Fractals* 44:160–168, 2011.
  - <sup>26</sup>Stephen, D. G., and A. Hajnal. Transfer of calibration between hand and foot: functional equivalence and fractal fluctuations. *Attent. Percept. Psychophys.* 73:1302–1328, 2011.
  - <sup>27</sup>Stephen, D. G., N. Stepp, J. A. Dixon, and M. T. Turvey. Strong anticipation: sensitivity to long-range correlations in synchronization behavior. *Phys. A* 387:5271–7278, 2008.

- <sup>28</sup>Stephen, D. G., B. Wilcox, J. B. Niemi, J. D. Franz, D. C. Kerrigan, and S. E. D'Andrea. Baseline-dependent effect of noise-enhanced insoles on gait variability in healthy elderly walkers. *Gait Posture* 36:537–540, 2012.
- <sup>29</sup>Stoffregen, T. A., C.-M. Yang, and B. G. Bardy. Affordance judgments and nonlocomotory body movements. *Ecol. Psychol.* 17:75–104, 2005.
- <sup>30</sup>Suki, B. Fluctuations and power laws in pulmonary physiology. *Am. J. Respir. Crit. Care Med.* 166:133–137, 2002.
- <sup>31</sup>Teich, M. C., C. Heneghan, S. B. Lowen, T. Ozaki, and E. Kaplan. Fractal character of the neural spike train in the visual system of the cat. *J. Opt. Soc. Am. A* 14:529–546, 1997.
- <sup>32</sup>Turcotte, D. L., B. D. Malamud, F. Guzzetti, and P. Reichenbach. Self-organization, the cascade model, and natural hazards. *Proc. Natl. Acad. Sci.* 19:2463–2465, 2002.
- <sup>33</sup>Turvey, M. T. Action and perception at the level of the synergies. *Hum. Mov. Sci.* 26:657–697, 2007.
- <sup>34</sup>Turvey, M. T., and C. Carello. Obtaining information by dynamic (effortful) touching. *Phil. Trans. R. Soc. B* 366:3123–3132, 2011.
- <sup>35</sup>Zheng, Y., J. Gao, J. C. Sanchez, J. C. Principe, and M. S. Okun. Multiplicative multifractal modeling of human neuronal activity. *Phys. Lett. A* 344:253–264, 2005.